This supplement provides details on the MFA models (Appendix A), the parameter selection (Appendix B), and additional experimental results (Appendix C).

A Details on MFA Models

To fit an MFA model, a set of points is given with function values observed at each point. Based on the mathematical formulations of Sec. 4, we use MFA models of degree 4 ($p = 4$). We then tackle the following key question: given an MFA model as the input, how can we extract topological descriptors from the model, without resorting to discretization or sampling?

In Tab. 1, we describe the MFA models representing four synthetic (left) and five scientific datasets (right); in particular, we list the number of spans used in each model.

Table 1: Details on the MFA models: the number of spans (#Span) used in each model.

Model	#Span	Model	#Span
Schwefel	71×71	S3D	136×104
Gaussian Mixture	46×71	Von Kármán	156×16
Sinc	27×27	Boussinesq	46×146
Gaussian Pair	17×11	CESM	200×100
		Hurricane Isabel	162×162

Schwefel MFA model. The (scaled) Schwefel function is a non-convex benchmark function that can be defined in any dimension [11]. In the 2D case, for a vector $\mathbf{x} = (x_1, x_2)^\top$, the function is defined as:

$$f(\mathbf{x}) = \frac{1}{2}\left(418.9829d - x_1 \sin(\sqrt{|x_1|}) - x_2 \sin(\sqrt{|x_2|})\right). \tag{1}$$

We create the Schwefel MFA model by fitting an MFA to a 2D Schwefel function within the domain $\left[-(10.5\pi)^2, (10.5\pi)^2\right]^2$.

Gaussian Mixture MFA model. The function associated with a synthetic Gaussian mixture [9] is defined as

$$\begin{aligned} f(\mathbf{x}) =& \exp\left[-8(x_1+0.4)^2 - 4x_2^2\right] + \exp\left[-8(x_1-0.5)^2 - 4x_2^2\right] \\ &+ \exp\left[-8x_1^2 - 4(x_2-0.77)^2\right] \qquad (2) \\ &+ \exp\left[-8x_1^2 - 4(x_2-1.5)^2\right] \\ &+ 0.2\exp\left[-0.3x_1^2 - 0.3(x_2-0.5)^2\right], \qquad (3) \end{aligned}$$

for $\mathbf{x} = (x_1, x_2)^\top$. To generate the Gaussian mixture MFA model, we fit an MFA to the original function in the domain $[-1, 1] \times [-0.8, 2.3]$.

Sinc MFA model. We define a synthetic functions of $\mathbf{x} = (x_1, x_2)^\top$ by adding Sinc functions in each dimension:

$$f(\mathbf{x}) = \frac{sin(5x_1)}{x_1} + \frac{sin(5x_2)}{x_2}. \tag{4}$$

To generate the Sinc MFA model, we fit an MFA to $f(\mathbf{x})$ in the domain $[-2\pi, 2\pi]^2$.

Gaussian Pair MFA model. We define a pair of synthetic functions of $\mathbf{x} = (x_1, x_2)^\top$, one is a Gaussian function, the other is a mixture of two Gaussian functions:

$$\begin{aligned} f(\mathbf{x}) =& 0.25 \cdot \exp\left[-\frac{(x_1-0.5)^2}{0.02} - \frac{(x_2-0.4)^2}{0.02}\right], \\ g(\mathbf{x}) =& 0.25 \cdot \exp\left[-\frac{(x_1-0.3)^2}{0.02} - \frac{(x_2-0.2)^2}{0.02}\right] \qquad (5) \\ &+ 0.25 \cdot \exp\left[-\frac{(x_1-0.75)^2}{0.02} - \frac{(x_2-0.25)^2}{0.0288}\right]. \end{aligned}$$

To generate the Gaussian Pair MFA model, we fit an MFA to the original functions in the domain $[0.1, 0.9] \times [0.0, 0.6]$. The MFA model represents f and g using the same spans but with different control points.

S3D MFA model. The dataset originates from an S3D turbulent combustion simulation [2], which simulates the interaction between a fuel jet combustion and an external cross-flow [3,4,7]. We use the magnitude of the 3D velocity field as the scalar function of interest. We extract a 2D slice from the dataset (defined on a grid) and fit an MFA model to it, which we refer to as the S3D MFA model.

Von Kármán Vortex Street MFA models. We work with a simulated von Kármán vortex street dataset [5, 10]. It originates from a simulation of a viscous 2D flow around a cylinder, capturing velocity fields over 1501 time steps. For the Jacobi set computation, we use the flow velocity magnitudes from two consecutive time steps as scalar fields f and g defined on a 2D grid. Specifically, we focus on time steps 1500 and 1501, where the vortex street is fully developed. We fit two MFA models to f and g respectively, which we refer to as the Von Kármán Vortex Street MFA models.

Boussinesq Approximation MFA model. The Boussinesq approximation dataset simulates a 2D flow generated by a heated cylinder [5, 10]. It consists of 2001 time steps. For the Jacobi set computation, we use the flow velocity magnitudes from time steps 2000 and 2001 as scalar fields f and g. We replace these scalar fields with MFA models as the surrogates.

CESM MFA model. The Community Earth System Model (CESM) provides extensive global climate data [8]. In our experiment, we focus on the FLDSC variable, which records the clear-sky downwelling long-wave flux on the surface, as modeled by the Community Atmosphere Model (CAM) developed at the National Center for Atmospheric Research (NCAR) [8]. We fit an MFA model to this dataset as the surrogate.

Hurricane Isabel MFA model. The Hurricane Isabel dataset generated using the Weather Research and Forecast (WRF) model [1] provides a collection of 3D scalar fields and a velocity vector field. These fields are defined over 48 time steps. For our analysis, we focus on the scalar fields of temperature and pressure at time step 30 with height 50. As shown in [6], at the height of 50, the hurricane exhibits significant spatial expansion and displays many characteristic structures. We again fit an MFA model to this dataset as the surrogate.

B Parameter Selection

Recall that we select our parameters—step size s, accuracy threshold ϵ, and trajectory connection threshold γ—based on a series of ablation studies. The *span length* l is the distance in the MFA model between knots and corresponding control points. All the MFA models in this study have a uniform span length across the entire model.

We first discuss the selection of step size s for particle tracing and the number of initial points needed to find starting points for particle tracing.

Step size. Particle tracing is performed independently within each span. To ensure particle tracing can be performed in every span, the step size s must satisfy $s \leq \frac{l}{2}$. To determine the proper step size, we run a series of experiments with different step sizes across each MFA model. In particular, we decrease step size $s \in \{l/2, l/4, l/8, \ldots, l/2^p, \ldots\}$ until both #Loop (the number of loops) and #CC (the number of connected components) reach convergence.

For experiments involving synthetic MFA models, as shown in Figs. 1 to 4, 8 and 12, both #Loop and #CC converge when $s = l/4$. Therefore, we set the step size $s = l/4$. On the other hand, scientific MFA models exhibit greater variability, so we select an optimal step size individually for each model-task pair based on analogous convergence criteria. The chosen step sizes are summarized in Tab. 2.

Table 2: Step sizes for MFA model-task pairs.

MFA Model	Step Size s
Schwefel (Contour)	$l/4$
Sinc (Contour)	$l/4$
Gaussian Pair (Jacobi set)	$l/4$
Gaussian Mixture (Ridge-valley graph)	$l/4$
S3D (Contour)	$l/16$
Kármán (Jacobi set)	$l/32$
Boussinesq (Jacobi set)	$l/32$
CESM (Ridge-valley graph)	$l/32$
Hurricane (Jacobi set)	$l/64$

Number of initial points for particle tracing. Particle tracing for contour extraction requires a set of starting points. In each span, MFA is a polynomial function and there could be multiple trajectories belonging to different parts of the same contour. We aim to find at least one starting point for each trajectory. We use gradient descent to locate the starting points (i.e., roots of polynomial functions) from a set of initial points. The contour at a fixed isovalue is a continuous curve that contains infinite number of points; in practice, we could only sample a finite set of starting points for trajectories within a span and connect them across spans.

For an MFA model, as the degree p increases, the contours could become more complex. To account for this, we set the number of initial points to be $(p+3)^2$ for a polynomial of degree p. Specifically, in each dimension, we select $(p+3)$ initial points: two points placed on the boundary and $(p+1)$ points sampled uniformly. We assume that this sampling strategy allows us to find at least one starting point on each trajectory through gradient descent.

When extracting the Jacobi set $\mathbb{J}(f,g)$, we convert the problem to a contour extraction at isovalue 0 of function h. The degree of h depends on degrees of f and g and is given by $p_h = p_f + p_g - 1$. Therefore, we set the number of initial points for Jacobi set extraction to be $(p_h+3)^2 = (p_f+p_g+2)^2$.

Similarly, for ridge-valley graph extraction, we convert it to a contour extraction problem at isovalue 0 of $\tilde{h}$. The degree of $\tilde{h}$ is $p_{\tilde{h}} = 3p_f - 1$. Consequently, we set the number of initial points to be $(p_{\tilde{h}}+3)^2 = (3p_f+2)^2$.

Accuracy threshold. We control contour extraction accuracy via a tolerance ϵ, so that points satisfy: $f(x) - a \leq \epsilon$. Both the Jacobi set and the ridge–valley graph can be reformulated as level 0 contour extraction problems; their accuracies are similarly governed by tolerances $h \leq \epsilon$ and $\tilde{h} \leq \epsilon$, respectively. To determine an appropriate value, we evaluate $\epsilon \in \{10^{-6}, 10^{-8}, 10^{-10}, 10^{-12}\}$ across all MFA models. According to the following ablation study, we find that $\epsilon = 1e^{-10}$ consistently provides sufficient precision, and thus use it for all our experiments.

Trajectory connection threshold. We connect trajectories whose endpoints are within a connection threshold γ. Since the step size determines the spacing between points, it also influences the distance between trajectories. Therefore, we evaluate $\gamma \in \{s, 1.5s, 2.0s, 2.5s\}$ across all MFA models. Based on results from synthetic models, we find that $\gamma = 2s$ is a suitable choice for achieving correct connectivity.

B.1 Ablation Study

Schwefel: contour extraction. We extract contours from the Schwefel MFA model at two isovalues, $a = 100$ and 500 respectively. According to the convergence plots in Figs. 1 and 2, our method accurately recovers the ground truth when $s \leq l/4$. Fixing $s = l/4$, we further investigate the sensitivity of the contour extraction algorithm w.r.t. parameters ϵ and γ. We use $\epsilon = 1.0e^{-10}$ and $\gamma = 2.0s$ in our experiment based on these convergence plots.

Sinc: contour extraction. We perform contour extraction at different isovalues $a = 0.33$ (Fig. 3) and $a = 0.79$ (Fig. 4). Based on the observed convergence behavior, we choose a step size of $s = l/4$. Additionally, we set $\epsilon = 1.0e^{-10}$ and $\gamma = 2.0s$ based on these convergence plots.

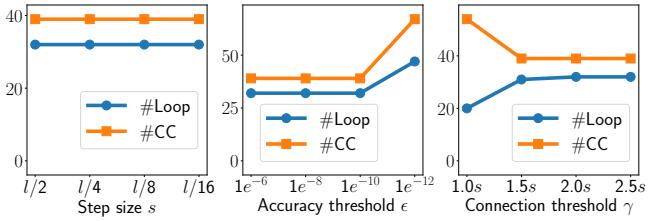

Figure 1: Schwefel model: Contour extraction at $a = 100$.

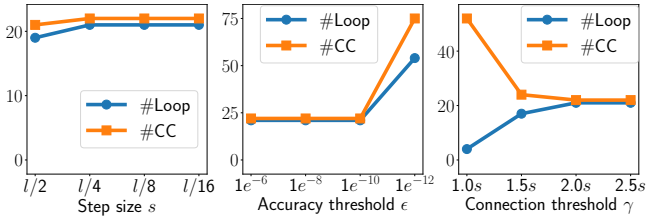

Figure 2: Schwefel model: Contour extraction at $a = 500$.

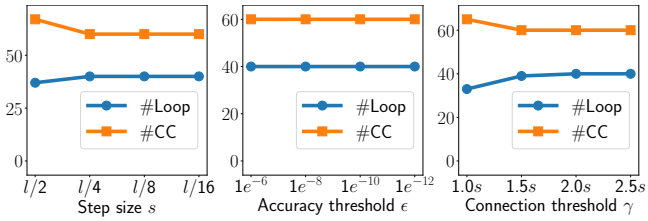

Figure 3: Sinc model: Contour extraction at $a = 0.33$.

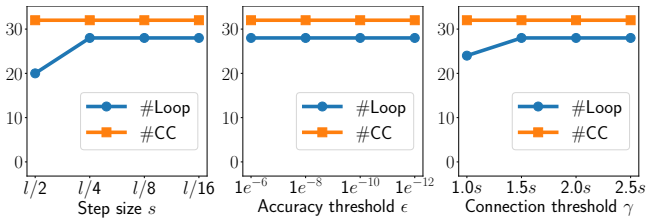

Figure 4: Sinc model: Contour extraction at $a = 0.79$.

S3D: contour extraction. We perform contour extraction at three different isovalues $a = 30$ (Fig. 5), $a = 50$ (Fig. 6), and $a = 60$ (Fig. 7). In these experiments, we adopt $s = l/16$, as both #Loop and #CC begin to stabilize at this point. These convergence plots also demonstrate the robustness of the accuracy threshold ϵ. Consistent with all other experiments, we use $\epsilon = 1.0e^{-10}$ and $\gamma = 2.0s$.

Gaussian Pair: Jacobi set extraction. Fig. 8 displays convergence plots of #Loop and #CC for step size, showing convergence starting from $s = l/4$. These plots also show stable convergence for $\epsilon \leq 1.0 \times 10^{-10}$. Moreover, the plots demonstrate the robustness of extraction results w.r.t. variations in the trajectory connection threshold γ.

Von Kármán Vortex Street: Jacobi set extraction. Fig. 9 presents convergence plots for varying step sizes. We use $s = l/32$, marking the onset of convergence. Convergence remains stable for $\epsilon \leq 1.0 \times 10^{-8}$. Additionally, these plots demonstrate the robustness of extraction results against variations in the trajectory connection threshold γ.

Hurricane Isabel: Jacobi set extraction. Similar to previous MFA models, convergence plots are shown in Fig. 10. The chosen

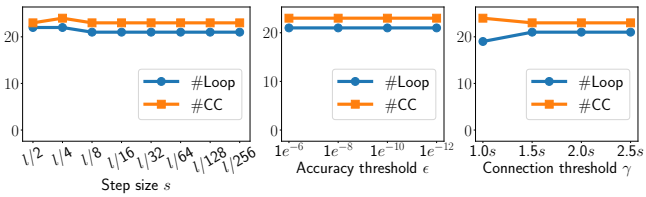

Figure 5: S3D model: Contour extraction at $a = 30$.

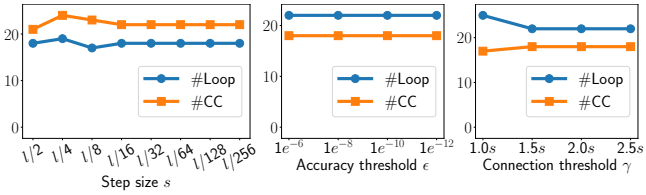

Figure 6: S3D model: Contour extraction at $a = 50$.

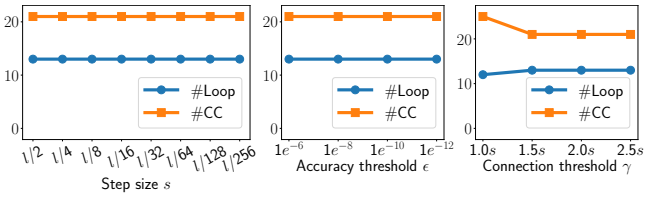

Figure 7: S3D model: Contour extraction at $a = 60$.

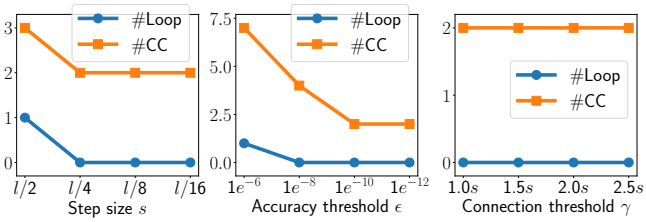

Figure 8: Gaussian pair model: Jacobi set extraction.

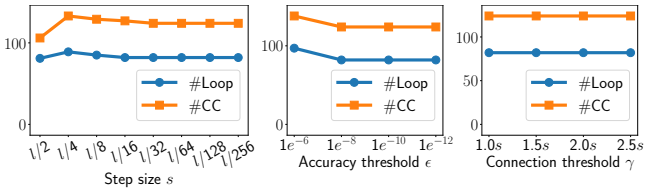

Figure 9: Von Kármán Vortex Street model: Jacobi set extraction.

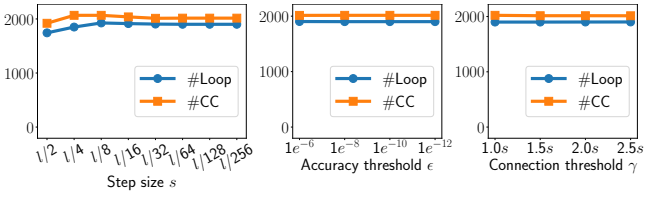

Figure 10: Hurricane Isabel model: Jacobi set extraction.

step size is $s = l/64$. These plots demonstrate that our extracted results are robust w.r.t. variations in ϵ and γ.

Boussinesq Approximation: Jacobi set Extraction. Fig. 11 shows convergence plots of Jacobi set extraction with various step sizes. Our experiments use $s = l/32$, $\epsilon = 1.0e^{-10}$, and $\gamma = 2.0s$.

Gaussian Mixture: ridge-valley graph extraction. We illustrate convergence plots for ridge-valley graph extraction in Fig. 12. A step size of $s = l/4$ is employed. In this experiment, a large γ may introduce additional loops; this effect is illustrated in the case of $\gamma = 2.5s$. We set $\epsilon = 1.0e^{-10}$ and $\gamma = 2.0s$ in our experiment.

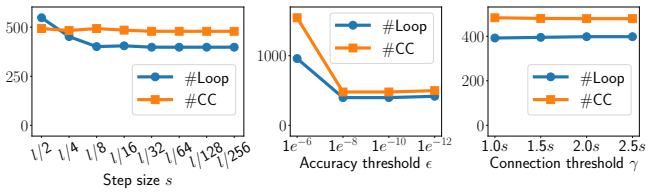

Figure 11: Boussinesq Approximation model: Jacobi set extraction.

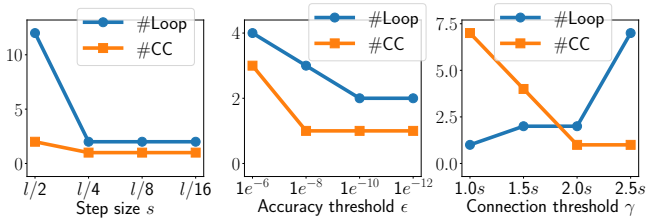

Figure 12: Gaussian mixture model: Ridge-valley graph extraction.

CESM: ridge-valley graph extraction. We show the convergence plots in Fig. 13. The step size is chosen to be $s = l/32$. Additionally, we set $\epsilon = 1.0e^{-10}$ and $\gamma = 2.0s$.

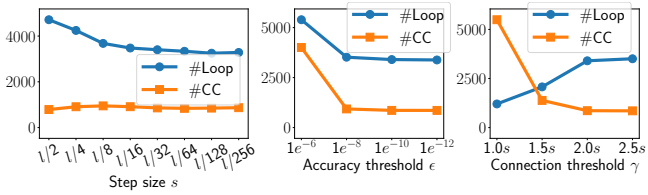

Figure 13: CESM model: Ridge-valley graph extraction.

C Additional Experimental Results

C.1 Schwefel: Contour Extraction

As shown in Fig. 14, we extract contours from the Schwefel MFA model with isovalues $a = 100$ and $a = 500$. Since the closed-form function that the Schwefel model approximates is known, we use it as the ground truth. In Tab. 3, all errors are below $\epsilon = 1e^{-10}$. Additionally, the number of loops and connected components matches that of the ground truth.

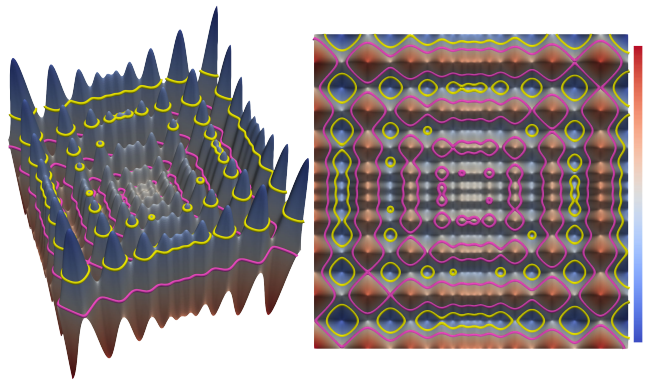

Figure 14: Schwefel model: contour extraction with isovalues $a = 100$ (yellow) and $a = 500$ (pink), shown from side and top viewpoints.

C.2 Boussinesq Approximation: Jacobi Set Extraction

In Fig. 15, we display the Boussinesq approximation model at time step 2000, with the extracted Jacobi set highlighted in yellow using step size $s = l/32$. Because our framework operates on a

Table 3: Schwefel model: Evaluation of contour extraction with various isovalues (a). GT denotes the ground truth.

a	$e_{\max}$	e_{avg}	#Loop	GT#Loop	#CC	GT#CC
100	$9.9e^{-11}$	$3.5e^{-12}$	32	32	39	39
500	$1.0e^{-10}$	$3.5e^{-12}$	21	21	22	22

continuous representation, the results remain smooth; see blocks (1). In contrast, the discrete method produces zigzag patterns; see block (2). The evaluation metrics in Tab. 4 indicate that the discrete method generates a large number of spurious loops.

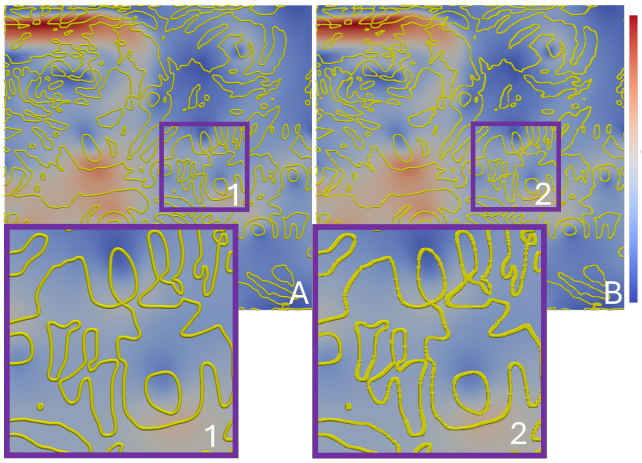

Figure 15: Boussinesq approximation model: Jacobi set extraction using MFA continuous method (A) and discrete method (B). (1) and (2): zoomed-in views of the purple blocks in (A) and (B), respectively.

Table 4: Boussinesq approximation model: Jacobi set extraction of MFA models with step size $s = 1/32$ and sampling ratio 32.

MFA Continuous Method				Discrete Method			
$e_{\max}$	e_{avg}	#Loop	#CC	$e_{\max}$	e_{avg}	#Loop	#CC
$1.0e^{-10}$	$1.6e^{-11}$	398	479	10.3	$2.7e^{-2}$	43888	9651

REFERENCES

[1] Hurricane Isabel. https://www.earthsystemgrid.org/dataset/isabeldata.html. Accessed: 2025-6-16. 1

[2] J. H. Chen, A. Choudhary, B. De Supinski, M. DeVries, E. R. Hawkes, S. Klasky, W. Liao, K. Ma, J. Mellor-Crummey, N. Podhorszki, R. Sankaran, S. Shende, and C. S. Yoo. Terascale direct numerical simulations of turbulent combustion using S3D. *Computational Science & Discovery*, 2(1):015001, 2009. doi: 10.1088/1749-4699/2/1/015001 1

[3] T. Fric and A. Roshko. Vortical structure in the wake of a transverse jet. *Journal of Fluid Mechanics*, 279:1–47, 1994. doi: 10.1017/S0022112094003800 1

[4] R. Grout, A. Gruber, C. S. Yoo, and J. Chen. Direct numerical simulation of flame stabilization downstream of a transverse fuel jet in cross-flow. *Proceedings of the Combustion Institute*, 33(1):1629–1637, 2011. doi: 10.1016/j.proci.2010.06.013 1

[5] T. Günther, M. Gross, and H. Theisel. Generic objective vortices for flow visualization. *ACM Transactions on Graphics (TOG)*, 36(4), 2017. doi: 10.1145/3072959.3073684 1

[6] D. Klötzl, T. Krake, Y. Zhou, I. Hotz, B. Wang, and D. Weiskopf. Local bilinear computation of Jacobi sets. *The Visual Computer*, 38(9):3435–3448, Sept. 2022. doi: 10.1007/s00371-022-02557-4 1

[7] G. Ma, D. Lenz, T. Peterka, H. Guo, and B. Wang. Critical point extraction from multivariate functional approximation. *2024 IEEE Topological Data Analysis and Visualization (TopoInVis)*, pp. 12–22, Oct. 2024. doi: 10.1109/TopoInVis64104.2024.00006 1

[8] R. B. Neale, C.-C. Chen, A. Gettelman, P. H. Lauritzen, S. Park, D. L. Williamson, A. J. Conley, R. Garcia, D. Kinnison, J.-F. Lamarque, D. Marsh, M. Mills, A. K. Smith, S. Tilmes, H. Morrison, P. Cameron-Smith, W. D. Collins, M. J. Iacono, R. C. Easter, S. J. Ghan, X. Liu, P. J. Rasch, and M. A. Taylor. Description of the NCAR community atmosphere model (cam 5.0). *NCAR Technical Note NCAR/TN-486+STR, National Center for Atmospheric Research, Boulder, Colorado, USA*, 2010. 1

[9] G. Norgard and P.-T. Bremer. Ridge–valley graphs: Combinatorial ridge detection using Jacobi sets. *Computer Aided Geometric Design*, 30(6):597–608, 2013. Foundations of Topological Analysis. doi: 10.1016/j.cagd.2012.03.015 1

[10] S. Popinet. Free computational fluid dynamics. *ClusterWorld*, 2(6):7, 2004. 1

[11] H.-P. Schwefel. *Numerical optimization of computer models*. John Wiley & Sons, Inc., USA, 1981. 1